Optical characterization of thin epitaxial GaAs films on Ge substrates

Cite as: J. Appl. Phys. **106**, 023505 (2009); https://doi.org/10.1063/1.3173282
Submitted: 06 March 2009 . Accepted: 10 June 2009 . Published Online: 16 July 2009

J. D. Wu, Y. S. Huang, G. Brammertz, and K. K. Tiong

Optical characterization of thin epitaxial GaAs films on Ge substrates

J. D. Wu,[1] Y. S. Huang,[1,a)] G. Brammertz,[2] and K. K. Tiong[3]
[1]*Department of Electronic Engineering, National Taiwan University of Science and Technology, Taipei 106, Taiwan*
[2]*Interuniversity Microelectronics Center (IMEC vzw), Kapeldreef 75, B-3001 Leuven, Belgium*
[3]*Department of Electrical Engineering, National Taiwan Ocean University, Keelung 202, Taiwan*

(Received 6 March 2009; accepted 10 June 2009; published online 16 July 2009)

Two thin epitaxial GaAs films on Ge substrates were characterized by photoluminescence (PL), contactless electroreflectance (CER), and piezoreflectance (PzR) techniques. The GaAs films containing antiphase domains (APDs) and those APD free were grown at 650 °C by metal organic vapor phase epitaxy. The PL intensity of the APD-containing film is four orders of magnitude lower than that of the APD-free sample. The reduction in intensity is due to the electrically active Ga–Ga and As–As bonds at the boundaries between the different APDs. The electric fields deduced from Franz–Keldysh oscillations of the CER spectra were used to determine the net carrier concentration of the GaAs films. In addition, the conduction to light-hole band transitions and the conduction to heavy-hole band transitions that originated from strain induced valence band splitting in GaAs thin films were observed and identified through a comparison of the relative intensities of light- and heavy-hole related features in the PzR and CER spectra. The results demonstrate that PL, CER, and PzR are useful nondestructive tools to characterize thin epitaxial GaAs films on Ge substrates.
 [DOI: 10.1063/1.3173282]

I. INTRODUCTION

As Si device scaling for future generations of complementary metal-oxide semiconductor (CMOS) circuits becomes increasingly difficult,[1] an alternative option becomes more and more appealing: GaAs and Ge are intrinsically faster semiconductors than Si, and especially the integration of a Ge *p*-type metal-oxide semiconductor with a GaAs *n*-type metal-oxide semiconductor is a very attractive replacement for fast Si CMOS structures.[2,3] Recently, a growing research interest in GaAs (Refs. 4 and 5) and Ge (Ref. 6) MOS transistor structures was observed for exactly that reason. For the cointegration of GaAs and Ge MOS structures in a planar scalable technology, very thin GaAs epitaxy on Ge is a key requirement. GaAs on Ge film thickness smaller than 100 nm can be achieved with very good epitaxial properties. Unfortunately, for such a small film thickness, many characterization techniques, such as x-ray diffraction, have reached their limit, whereas other characterization techniques, such as transmission electron microscopy, are very costly and time consuming.

In this work, we have employed photoluminescence (PL), contactless electroreflectance (CER), and piezoreflectance (PzR) techniques to characterize two GaAs films with a thickness of ~1 μm. These optical diagnostic tools are effective as rapid and easy methods to assess the quality of thin GaAs layers on Ge substrates. The methods are nondestructive and can yield information about the structural quality of the material as well as information on the doping materials and concentration. Both antiphase domain (APD)-containing and APD-free GaAs films were grown at 650 °C by metal organic vapor phase epitaxy (MOVPE). The PL intensity of the APD-free film is much larger than that of the APD-containing sample. The PL spectra at low temperatures show the splitting of the band to band recombination peaks, indicating the existence of strain in the GaAs thin film. The CER spectra show the Franz–Keldysh oscillations (FKOs) above the band gap of GaAs. The built-in electric fields, as determined from the observed FKOs, can be used to evaluate the net carrier concentration of the GaAs films. By a comparison of the relative intensities of PzR and CER spectra, the identification of the conduction to light-hole (LH) band transitions and the conduction to heavy-hole (HH) band transitions that originated from the strain induced valence band splitting has been achieved. The results demonstrate that PL, CER, and PzR are useful nondestructive tools to characterize thin epitaxial GaAs films on Ge substrates.

II. EXPERIMENTAL

Two GaAs films with a thickness of 1 μm employed in this study were grown on Ge(001) substrates using MOVPE in a Thomas Swan reactor. *n*-type Ge substrates with a miscut angle of 0°/6° off (001) toward [111] were used to grow APD-containing (sample A)/APD-free (sample B) GaAs epitaxial layers. The films were covered with a 20 nm AlAs layer in order to prevent surface recombination. The precursor sources were trimethylgallium, tertiarybutylarsin, silane as an *n*-type dopant, and palladium-purified H_2 as a carrier gas. The growth temperature was 650 °C. The reciprocal space maps of the films indicated that the GaAs layers are fully stressed.[7]

PL spectra were excited using a double frequency 100 mW yttrium aluminum garnet:Nd laser (532 nm). The luminescence signals were analyzed using a Jobin-Yvon "TRIAX 550" spectrometer equipped with a "Symphony" charge

a)Author to whom correspondence should be addressed. Electronic mail: ysh@mail.ntust.edu.tw.

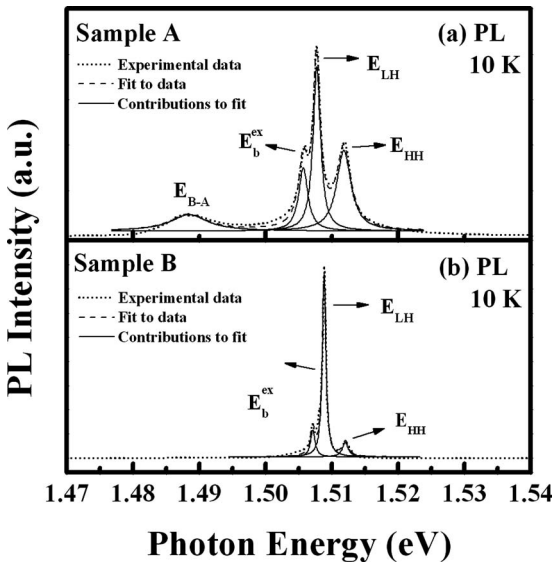

FIG. 1. The 10 K PL spectra (dotted lines) in the range of 1.46–1.54 eV for (a) the APD-containing (sample A) and (b) APD-free (sample B) GaAs epilayers grown on Ge substrates. The fits to the experimental data are shown as well (dashed lines). The solid lines show the different components of the fits.

coupled device camera. In the CER experiment, an ac modulating voltage (~1 kV at 200 Hz) was applied between a front wire grid electrode and a second electrode consisting of a metal plate. These two electrodes were separated by an insulating spacer in such a manner that there was a very thin layer (~0.1 mm) of air (or vacuum) between the front surface of the sample and the front electrode. Thus, there is no direct contact with the front surface of the sample. The probe beam enters through the front wire grid. For the PzR measurements, the thin samples were glued on a 0.15 cm thick lead zirconate titanate piezoelectric transducer driven by a 200 V_{rms} sinusoidal source at 200 Hz. The alternating expansion and contraction of the transducer subjected the sample to an alternating strain with a typical rms $\Delta l/l$ value of $\sim 10^{-5}$. The radiation from a 150 W tungsten-halogen lamp filtered by a 0.25 m monochromator provided the monochromatic light. The reflected light was detected by a silicon photodiode. The dc output of this photodiode was maintained constant by a servomechanism of a variable neutral density filter. A dual-phase lock-in amplifier was used to measure the detected signals. Multiple scans over a given photon energy range were programed until a desired signal-to-noise level was attained with a computer controlled data acquisition procedure. Detailed CER and PzR configurations have been described elsewhere.[8,9] A closed-cycle cryogenic refrigerator equipped with a digital thermometer controller was used for the low temperature measurements with a temperature stability of 0.5 K or better.

III. RESULTS AND DISCUSSION

Figures 1(a) and 1(b) show, respectively, the 10 K PL spectra in the range of 1.46–1.54 eV measured with a spectrometer resolution of 0.05 meV for the APD-containing (sample A) and APD-free (sample B) GaAs epilayers grown on Ge substrates. It can be seen in Fig. 1(a) that there are three sharp features located at 1.5118, 1.5077, and 1.5057 eV with full widths at half maximum (FWHMs) of 2.6, 1.4, and 1.7 meV in the band to band region and a broader structure at 1.4884 eV for sample A. The peak at 1.4884 eV has been attributed to band to acceptor transitions, denoted as $E_{B\text{-}A}$, involving residual carbon impurities present in MOVPE GaAs.[10] The origins for the three near band edge recombination features are tentatively assigned as free HH (E_{HH}), free LH (E_{LH}), and bound excitonic transitions (E_b^{ex}). The splitting of the band to band peak into two separate peaks is due to valence band splitting into LH and HH components caused by stresses in the GaAs layer.

The epitaxial growth of GaAs on Ge can result in a built-in biaxial stress on GaAs due to a small difference between the lattice constants, GaAs (5.6533 Å)/Ge (5.658 Å), and thermal expansion coefficients of GaAs and Ge. The biaxial stress is expected to split the valence band degeneracy by producing the anisotropic deformation of the crystal lattice.[11,12] For the fundamental critical point transitions denoted as E_g, the hydrostatic component of the strain, δE_H, shifts the valence band of the GaAs relative to the conduction band, while the shear component, δE_S, removes the valence band degeneracy, giving a split E_{LH} and E_{HH}.[11,12] If the effect of the strain induced coupling with the spin-orbit split band is negligible, the split energy gaps can be expressed in terms of the unstrained value as[13]

$$E_{HH} = E_g + \delta E_H + \delta E_S, \tag{1}$$

$$E_{LH} = E_g + \delta E_H - \delta E_S. \tag{2}$$

The values of δE_H and δE_S are given in terms of the strain perpendicular to the (001) surface, ε, and the elastic stiffness constants, C_{ij}, by[13]

$$\delta E_H = 2a[(C_{11} - C_{12})/C_{11}]\varepsilon, \tag{3}$$

$$\delta E_S = -b[(C_{11} + 2C_{12})/C_{11}]\varepsilon, \tag{4}$$

where a and b are the hydrostatic and tetragonal shear deformation potentials, respectively, and $\varepsilon = (a_{Ge} - a_{GaAs})/a_{Ge}$. The numerical values of C_{11}, C_{12}, a, and b for GaAs are 118.8 GPa,[14] 53.2 GPa,[14] −8.7 eV,[15] and −2.0 eV,[15] respectively. Using these numerical values, the splitting between the LH and HH is calculated to be 6.3 meV. The identification of the LH and HH related features will be further discussed later.

As shown in Fig. 1(b), similar to that of sample A, there are three sharp features located at 1.5120, 1.5088, and 1.5071 eV with the FWHMs of 1.1, 0.6, and 0.8 meV in the band to band region and a weak broad structure at 1.489 eV for sample B. The splitting of the two higher energy features (the valence band splitting) is determined to be 3.2 ± 0.1 meV for sample B, which is found to be smaller than that of sample A (4.1 ± 0.1 meV), indicating that a smaller strain for the APD-free film was grown on 6° miscut Ge.

In order to show the full variation in the PL intensities of the two samples, the spectra are shown on a logarithmic scale and depicted in Fig. 2. It is clear that the effect of the APDs is to suppress most of the light emission from the GaAs films. As shown in Fig. 2, the PL intensity of the

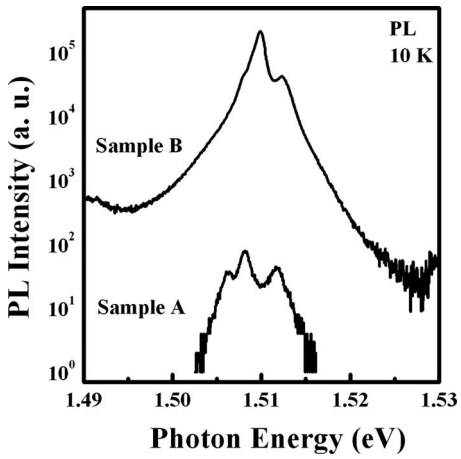

FIG. 2. A logarithmic scale of 10 K PL spectra for a GaAs layer deposited on 0° miscut Ge (APD-containing: sample A) and a GaAs film deposited on 6° miscut Ge (APD-free: sample B). The thickness of the films is 1 μm, and the films are covered with a 20 nm AlAs layer in order to prevent surface recombination.

APD-containing GaAs film is about four orders of magnitude lower than that of the APD-free one. This reduction in intensity is due to the electrically active Ga–Ga and As–As bonds at the boundaries between the different APDs, which acts as strong nonradiative recombination centers.

Shown in Fig. 3 are the CER spectra at 300 K for samples A (solid line) and B (dotted line). In the CER spectra, a set of subsidiary oscillations known as the FKOs can be observed above E_g. From the theory of modulation spectroscopy, the asymptotic behavior of FKOs can be described by[16]

$$\frac{\Delta R}{R} \propto [E^2(E-E_g)]^{-1} \exp[-2(E-E_g)^{1/2}\Gamma/(\hbar\theta)^{3/2}] \times \cos[4/3(E-E_g)^{3/2}/(\hbar\theta)^{3/2} + \phi]. \quad (5)$$

Here, E is the photon energy, E_g is the band gap, Γ is the broadening factor, and ϕ is a phase factor related to the interaction between electrons and holes, which can be determined by fitting the experimental data. The parameter $\hbar\theta$ is defined as[17]

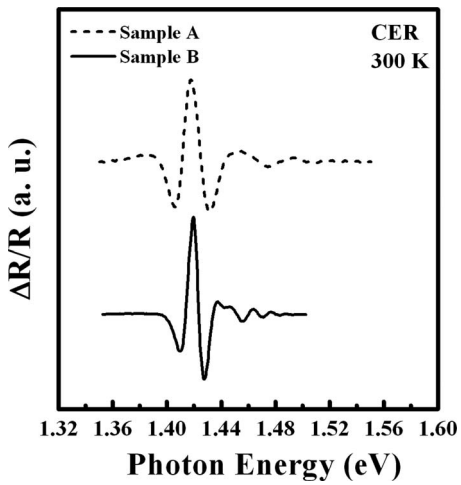

FIG. 3. The CER spectra at 300 K for APD-containing (sample A: solid line) and APD-free (sample B: dotted line) GaAs thin films grown on Ge substrates. The FKOs were observed above E_g.

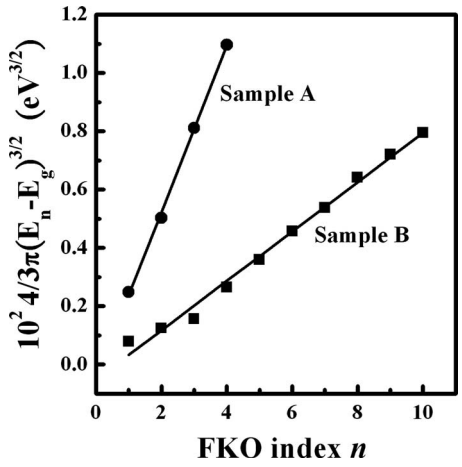

FIG. 4. Plots of $(4/3\pi)(E_n-E_g)^{3/2}$ vs index number n in accordance with the spectra in Fig. 3. The solid lines are least-squares fits to a linear function.

$$\hbar\theta = \left(\frac{e^2\hbar^2F^2}{2\mu}\right)^{1/3}, \quad (6)$$

where e is the charge of an electron, $\hbar$ is the Planck's constant divided by 2π, F is the strength of the electric field, and μ is the reduced mass of the electron and hole in the direction of the electric field. The extrema of the oscillations E_n above E_g are given approximately by[17]

$$n\pi = \phi + \frac{4}{3}\left(\frac{E_n-E_g}{\hbar\theta}\right)^{3/2}. \quad (7)$$

From the experimental data, a straight line plot of $(E_n-E_g)^{3/2}$ against n can be made. The slope of the straight line yields $\hbar\theta$, and hence the electric field F can be determined using Eq. (6).

The above relationship is originally derived from the theory of the dielectric function in uniform electric fields. For a linear electric field in a surface charge region at the semiconductor surfaces, it can be shown[17] that the electric field derived from Eq. (7) is approximately the maximum value of the field, i.e., the surface field F_s. For an n-type semiconductor, it has been shown that the carrier concentration N is proportional to square of the surface field F_s determined from FKOs with[18]

$$F_S = \left(\frac{2eN(V_{\text{bi}} - V_{\text{ext}} - kT/e)}{\varepsilon_0\varepsilon_s}\right)^{1/2}, \quad (8)$$

where V_{bi} is the built-in potential, V_{ext} is the external potential, N is the carrier concentration, k is the Boltzmann constant, ε_s is the static dielectric constant, and ε_0 is the free space permittivity.

Using the aforementioned theoretical consideration, a plot of the quantity $(4/3\pi)(E_n-E_g)^{3/2}$ as a function of n for the samples was performed and depicted in Fig. 4. The respective plots for samples A and B were linear fits to Eq. (7) to yield the corresponding values for $\hbar\theta$, which were then utilized to deduce the electric fields in the GaAs layer through the use of Eq. (6). The values of the effective masses

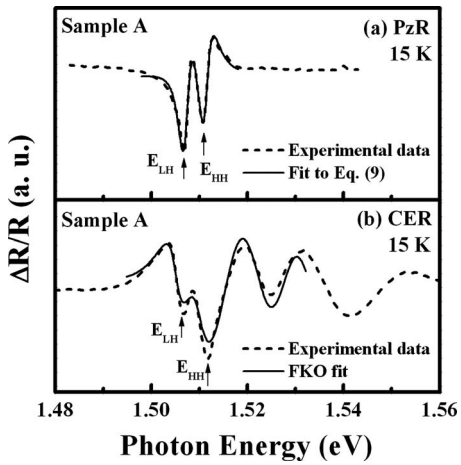

FIG. 5. (a) The experimental PzR data (dashed line) at 15 K of an APD-containing GaAs thin film grown on Ge substrate. The full curve is the least-squares fit to Eq. (9). (b) The experimental CER data (dashed line) at 15 K. The full curve is the FKO fit.

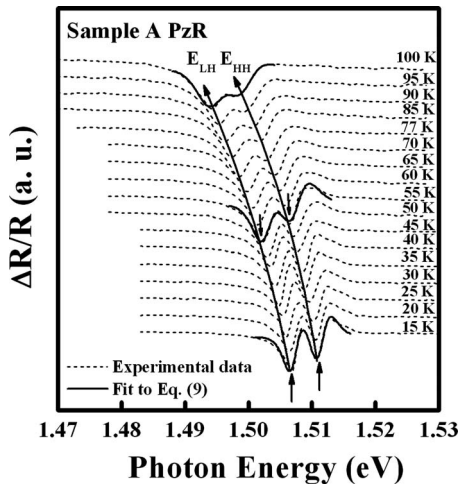

FIG. 6. The temperature dependent PzR spectra (dashed lines) in the range of 15–100 K. The full curves are the least-squares fits to Eq. (9). The obtained conduction to LH and HH transitions are denoted with arrows. The solid lines, guide to the eye, with arrows indicate the E_{LH} and E_{HH} shifts toward lower energies with increasing temperature.

are $m_e^*=0.067m_0$, $m_{HH}^*=0.34m_0$, and $m_{LH}^*=0.08m_0$.[19] From the analysis, the values of $F=35\pm3$ kV/cm for sample A and $F=10\pm1$ kV/cm for sample B were evaluated.

As mentioned earlier, the evaluated values of F are close to the values of the surface field F_s. It is also known that for GaAs, the surface Fermi level is pinned around the midgap by surface states. We can then evaluate the carrier concentration N, which is proportional to the square of the surface field F_s determined from FKOs for the case of $V_{ext}=0$. The difference in the obtained electrical fields indicated that the background doping of the two samples differed by one order. The results were further confirmed by the capacitance-voltage (C-V) technique.

In order to identify the origin of near band edge splitting transitions, PzR and CER measurements were carried out. Figure 5(a) shows the PzR spectrum for sample A at 15 K. For comparison, the CER spectrum at 15 K is depicted in Fig. 5(b). As shown in Fig. 5(a), the dotted line denotes the experimental PzR data and the full curve denotes the least-squares fit to the derivative Lorentzian line shape function of the form[8,9]

$$\frac{\Delta R}{R}=\mathrm{Re}\sum_{j=1}A_j e^{i\Phi_j}(E-E_j+i\Gamma_j)^{-n}, \tag{9}$$

where A_j and Φ_j are the amplitude and phase of the line shape, E_j and Γ_j are the energy and broadening parameters of the transitions, and the value of n depends on the origin of the transitions. For derivative functional form, $n=2$ is appropriate for bound states such as excitons. As can be seen in Fig. 5(a), the line shape fits for the PzR spectrum clearly show two structures (indicated with arrows) near the band edge of GaAs. To identify the physical origin of the doublets, we make a spectral comparison of the PzR and CER measurements.

For the PzR measurement under [001]-symmetry coplanar stress, the intensity ratio between the conduction to LH band transitions and the conduction to HH band transitions has been shown to follow the relation[20]

$$K_{PzR}=\frac{dE_{LH}/dS}{dE_{HH}/dS}=\frac{a(2-\lambda)+b(1+\lambda)}{a(2-\lambda)-b(1+\lambda)}. \tag{10}$$

The variable S refers to the modulating stress applied to the sample. The parameters a and b represent the hydrostatic and the shear deformation potentials, respectively, and $\lambda=2C_{12}/C_{11}$, where C_{ij} is the elastic stiffness constants. We have used a number of relevant parameters from literatures for that of GaAs.[14] The ratio of K_{PzR} for GaAs is then evaluated to be about 2.2 from Eq. (10). This result indicates that the transition of LH is more sensitive than that of HH under the [001]-symmetry coplanar piezomodulation. To further confirm this observation, we have also studied the CER spectrum of the same sample. As shown in Fig. 5(b), the observed FKOs in the CER spectrum can be fitted with two FKOs (LH and HH related), where the transition energies, the amplitudes, and the built-in electric field were used as fitting parameters. The band edge energies, the period of FKOs, and its damping profile yield the information about the stress effect and the built-in electric field. The relative intensity of the LH and HH transitions for the CER measurements is insensitive to strain and has been used as a reference. The ratio $(dE_{LH}/dS)/(dE_{HH}/dS)$ is proportional to $(I_{LH}/I_{HH})_{PzR}$ in the PzR spectra and to $(I_{LH}/I_{HH})_{CER}$ in the CER spectra. In the strain-insensitive CER spectra, the modulation coefficient is the same for all transitions, so that the ratio $(I_{LH}/I_{HH})_{PzR}/(I_{LH}/I_{HH})_{CER}$ gives the ratio of the piezomodulation coefficients of the LH and HH transitions. From the PzR measurements for the GaAs film, the enlarged feature appeared at the lower energy side with respect to the HH feature, indicating the presence of a tensile-type stress in the sample. The K_{PzR} is determined to be 2.1 for sample A. The experimentally deduced values of K_{PzR} agreed reasonably well with those of the theoretical calculation.

Figure 6 depicts the temperature dependent PzR spectra in the range of 15–100 K. The spectra consist of two features and are fitted with Eq. (9). The obtained conductions to LH and HH transitions are denoted with arrows. The solid lines,

guide to the eye, with arrows indicate the E_{LH} and E_{HH} shifts toward lower energies with increasing temperature. The separation of these two features is found to be insensitive to the temperature variations. The results show similar thermal expansion coefficients for GaAs and Ge in the temperature range of 15–100 K, indicating that the biaxial stress is mainly due to a small difference in the lattice constants of GaAs and Ge.

IV. SUMMARY

In summary, we have characterized two thin epitaxial GaAs films, one containing APDs and one APD free, on Ge substrates deposited via MOVPE by using PL, CER, and PzR techniques. The PL spectra at low temperatures show the splitting of the band to band recombination peaks, indicating the existence of strain in the GaAs thin film. The PL intensity of the APD-containing film is four orders of magnitude lower than that of the APD-free sample. The reduction in intensity is due to the electrically active Ga–Ga and As–As bonds at the boundaries between the different APDs. The CER spectra show the FKOs above the band gap of GaAs. The built-in electric fields, as determined from the observed FKOs, are used to evaluate the net carrier concentration of the GaAs films. In addition, the conduction to LH band transitions and the conduction to HH band transitions that originated from strain induced valence band splitting in GaAs thin films are observed and identified through a comparison of the relative intensities of LH and HH related features in the PzR and CER spectra. The results demonstrate that PL, CER, and PzR are useful nondestructive tools to characterize thin epitaxial GaAs films on Ge substrates.

ACKNOWLEDGMENTS

The authors acknowledge the support of National Science Council of Taiwan under Project No. NSC 97-2221-E-011-131.

[1] M. Ieong, B. Doris, J. Kedzierski, K. Rim, and M. Yang, Science **306**, 2057 (2004).
[2] R. Chau, S. Datta, M. Doczy, B. Doyle, B. Jin, J. Kavalieros, A. Majumdar, M. Metz, and M. Radosavljevic, IEEE Trans. Nanotechnol. **4**, 153 (2005).
[3] G. Brammertz, M. Caymax, M. Meuris, M. Heyns, Y. Mols, S. Degroote, and M. Leys, Thin Solid Films **517**, 148 (2008).
[4] P. D. Ye, G. D. Wilk, B. Yang, J. Kwo, S. N. G. Chu, S. Nakahara, H.-J. L. Gossmann, J. P. Mannaerts, M. Hong, K. K. Ng, and J. Bude, Appl. Phys. Lett. **83**, 180 (2003).
[5] M. Passlack, R. Droopad, K. Rajagopalan, J. Abrokwah, R. Gregory, and D. Nguyen, IEEE Electron Device Lett. **26**, 713 (2005).
[6] E. J. Preisler, S. Guha, B. R. Perkins, D. Kazazis, and A. Zaslavsky, Appl. Phys. Lett. **86**, 223504 (2005).
[7] G. Brammertz, Y. Mols, S. Degroote, V. Motsnyi, M. Leys, G. Borghs, and M. Caymax, J. Appl. Phys. **99**, 093514 (2006).
[8] Y. S. Huang and F. H. Pollak, Phys. Status Solidi A **202**, 1193 (2005).
[9] F. H. Pollak and H. Shen, Mater. Sci. Eng. R. **10**, xv (1993).
[10] M. K. Hudait, P. Modak, S. Hardikar, and S. B. Krupanidhi, J. Appl. Phys. **83**, 4454 (1998).
[11] F. H. Pollak and M. Cardona, Phys. Rev. **172**, 816 (1968).
[12] F. H. Pollak, Surf. Sci. **37**, 863 (1973).
[13] S. L. Chuang, *Physics of Optoelectronic Devices* (Wiley, New York, 1995), p. 440.
[14] S. Adachi, J. Appl. Phys. **58**, R1 (1985).
[15] H. Qiang, F. H. Pollak, and G. Hickman, Solid State Commun. **76**, 1087 (1990).
[16] D. E. Aspnes and A. A. Studna, Phys. Rev. B **7**, 4605 (1973).
[17] H. Shen and F. H. Pollak, Phys. Rev. B **42**, 7097 (1990).
[18] Z. Wang, S. Pan, S. Huang, C. Zhang, S. Mu, X. Zhou, J. Jian, G. Xu, and Z. Chen, J. Phys. D: Appl. Phys. **26**, 1493 (1993).
[19] *Numerical Data and Functional Relationships in Science and Technology*, Landolt-Bornstein, New Series, Group III, Vol. 22, Pt. A, edited by O. Madelung and M. Schulz (Springer, New York, 1987).
[20] H. Mathieu, J. Allègre, and B. Gil, Phys. Rev. B **43**, 2218 (1991).